River Flow 2010 - Dittrich, Koll, Aberle & Geisenhainer (eds) - © 2010 Bundesanstalt für Wasserbau ISBN 978-3-939230-00-7

Hybrid modelling of dike-break induced flows

S. Roger, J. Köngeter & H. Schüttrumpf
Institute of Hydraulic Engineering and Water Resources Management (IWW), RWTH Aachen University, Hydraulic Laboratory Kreuzherrenstraße 7, 52056 Aachen, Germany

S. Erpicum, P. Archambeau & M. Pirotton
Department ArGEnCo, Research unit of Hydrology, Applied Hydrodynamics and Hydraulic Constructions (HACH), University of Liege, Chemin des Chevreuils 1 Bât. B52/3+1, 4000 Liege, Belgium

D. Schwanenberg
Deltares, Operational Water Management, Rotterdamseweg 185, 2629 HD Delft, NL

B.J. Dewals
Belgian Fund for Scientific Research F.R.S.-FNRS

ABSTRACT: In a hybrid approach experimental model data are combined with results from 3D and 2D numerical modelling. The latter was conducted by two different models solving the depth-averaged shallow water equations. 3D computations are based on the REYNOLDS-averaged NAVIER-STOKES equations (RANS) using a volume of fluid approach to capture the free water surface. Measurements were performed on a scale model which was especially designed to reproduce the specific conditions of dike breaks. In various simulations it turned out that 2D shallow water models are able to reproduce steady-state flow patterns of dike-break induced flows and that there is a low sensitivity of the solution concerning turbulence modelling, bed and wall roughness. Nevertheless, final flow splits and breach discharges are systematically underestimated. This discrepancy seems to result from inherent modelling assumptions such as zero-vertical velocity and hydrostatic pressure distribution. Therefore, the complementary use of 3D RANS and 2D depth-averaged modelling frameworks for detailed predictions of dike-break induced flows is discussed in the present paper, based on BOUSSINESQ and pressure coefficients, which represent effects of non-uniform velocity profiles and non-hydrostatic pressure distribution over water depth, respectively. Values of these coefficients are inferred from 3D numerical results for the final steady state.

Keywords: BOUSSINESQ coefficients, Discontinuous Galerkin, Finite volume, Dike break, Hybrid modelling

1 INTRODUCTION

1.1 *Motivation*

In case of a failure of flood protection measures (e.g. dikes, mobile walls) a wave is initiated into the hinterland and may cause extensive damage in densely populated floodplains. Recurring dike breaks at massive flood events indicate that inland flood protection is vulnerable and the resulting risk has to be assessed. A Risk Assessment procedure has been developed at the Institute of Hydraulic Engineering and Water Resources Management (IWW), RWTH Aachen University. The basic principle of this approach, which was originally developed for German dams by Rettemeier et al. (2000), can be transferred to rivers and dikes (Kutschera et al., 2008). Mathematically, the risk is obtained by multiplying the probability of a dike failure by the extent of the damage caused in the event of a collapse. To assess the risk provoked by floods and corresponding protective structures, the potential damage on people and property has to be determined, which involves the identification of inundated areas as well as flow depths and velocities of the initiated wave.

The static impact basically depends on the total water volume entering the hinterland over a long period. This state has to be considered when focussing on the long-term and large-scale inundation in the entire floodplain. The steady-state breach discharge through a collapsed dike section significantly affects final water levels and the extent of inundated areas, while during the first transient phase the combination of flow velocities and water depths within the dike-break wave induces dynamic damages nearby the breach location. Compared to the duration of the whole flood event this period is often short but equally dangerous for people and property in the affected region.

The results of dike-break induced flow computations are used to identify and illustrate areas of significant flood risk (flood mapping). Simulations of scenarios may also provide authorities

with valuable information like flood arrival time or main flow directions to manage the residual risk: definition of evacuation zones, coordination of civil protection, and land use planning.

1.2 *Phenomenon*

In contrast to the wide knowledge of flood wave propagation initiated by dam breaks (Hervouet & Petitjean 1999, Brufau & Garcia-Navarro 2000, CADAM 2000, Toro 2001, RESCDAM 2001, IMPACT 2005) the expertise of dike-break induced flows is not satisfactory. The latter are influenced by the main flow direction of the river parallel to the flood protection structure (asymmetric flood wave propagation). Moreover, unlike reservoirs at rest, a river bed will not be empty: the persisting flood discharge of the river leads to a fixed water level in the breach after a certain time (final steady state) resulting in a partition of the inflow into the downstream and the breach discharges, which partly corresponds to a withdrawal of water. A dike break may thus be classified between a dam break and a channel junction as illustrated in Figure 1.

The related flows can be characterized as large-scale, long-term but at the same time transient, 3D, turbulent and multiphase (air entrainment, sediment transport) flows with complex free-surface behaviour upon a heterogeneous topography (initially dry, geometrically complicated, covered by buildings and plants).

There is a lack of knowledge as regards these types of flood waves. The existing measured data are not sufficient due to the unpredictability, rareness and the danger of such events. The safety of threatened people and property as well as the security of the gauging staff during the event has priority, which complicates complex measuring campaigns close to a breach.

There exist only few investigations considering the propagation of a wave into an area, such as Fraccarollo & Toro (1995), Stelling & Duinmeijer (2003), Kulisch (2002), Shige-eda & Akiyama (2003), Aureli et al. (2004), and Eaket et al. (2005) relating to dam-break flows, however. Aureli & Mignosa (2002, 2004) only considered the presence of a permanent river discharge. That is why numerical models can not be properly validated and therefore may not calculate reliable simulation results for complex scenarios.

1.3 *Hybrid procedure*

Circumventing the expense of a full-sized prototype, a bench-scale model was used to provide experimental data, which were recorded with sophisticated measurement techniques to explore flow effects and to validate numerical models. In an *experimental model* natural phenomena are scaled down and idealised resulting in differences between modelled and real procedures. A *numerical model* contains simplifications in the mathematical description and numerical treatment of flow phenomena. To solve this problem, experimental and numerical models are combined in a hybrid approach to benefit from each other by exploiting their respective advantages and compensating their weak-points at the same time.

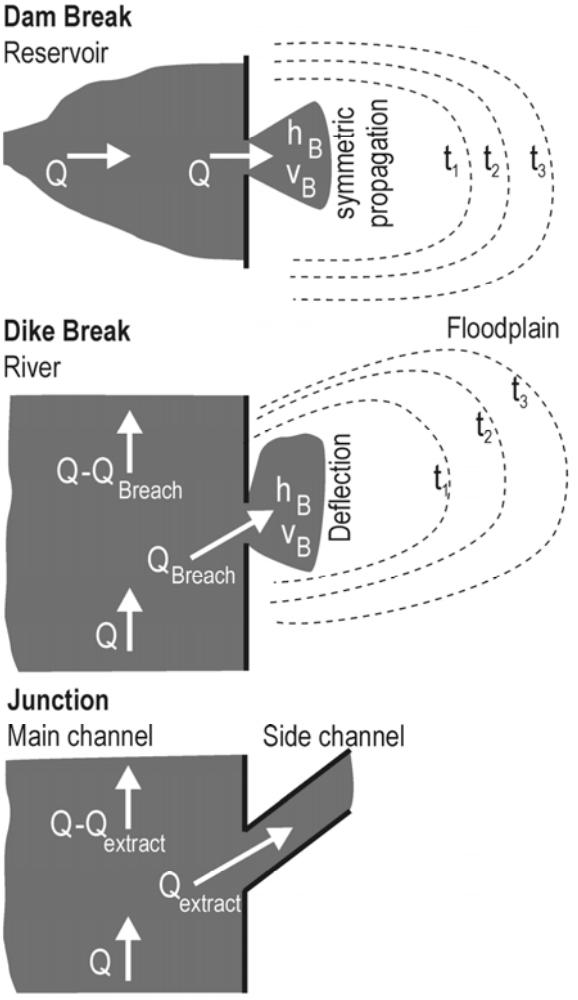

Figure 1. Classification of dike-break induced flows.

On the one hand, the accuracy of numerical forecasts can directly be quantified by measurements. On the other hand, numerical simulations complement the model tests by calculating scenarios of different configurations, geometries and boundary conditions. The combination enables selective improvements in numerical methods and more reliable forecasts for long-term and large-scale applications. The forecast quality is directly quantifiable by comparisons between simulation results (coming from different numerical schemes and mathematical approaches) and measured data in terms of flow discharges, water depths, flow velocities, and arrival times (depending on the fact whether the first dynamic phase or the final steady state is evaluated).

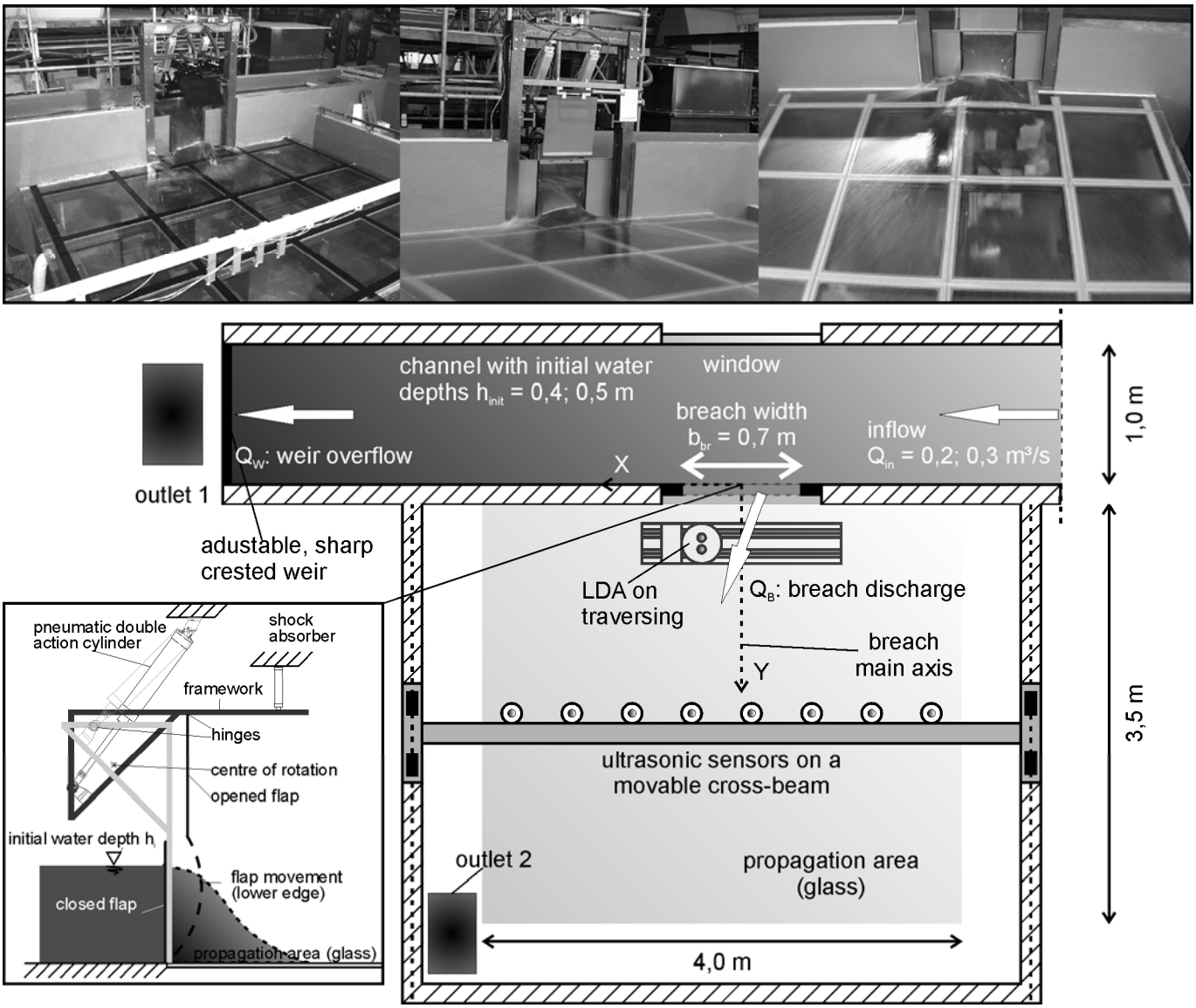

Figure 2. Scale model set-up.

2 EXPERIMENTAL MODEL

2.1 *Apparatus*

The idealised experimental set-up in Figure 2 takes into account specific boundary conditions of dike-break induced flows close to the breach section (Briechle & Köngeter, 2002, Briechle et al., 2004). It consists of a horizontal rectangular channel (width 1 m) with a pneumatically driven gate at one bank and an even adjacent flat propagation area (3.5 times 4.0 m²) made of glass. The entire opening of the flap gate takes less than 0.3 s, which represents the worst case scenario of a sudden and complete dike failure. Moreover, the opening mechanism is a combination of pull and rotation to minimize influence on the free water column when the wave is initiated. As opposed to straight flumes, the water propagates radial and falls off the glass plate freely at three edges. The bottom of the propagation area is made of glass to minimize roughness effects and to enable laser measurements from below the plate. Initial water levels in the channel (0.3 – 0.5 m), channel discharges (0.1 – 0.3 m³/s), and breach widths (0.3 – 0.7 m) could be varied.

2.2 *Measuring techniques*

Due to strong temporal and spatial variations of the initiated wave as well as air entrainment, an advanced non-intrusive measuring technique was necessary providing high frequencies and stability towards dynamically changing water levels. Thus, water depths were recorded by ultrasonic sensors with 25 Hz frequency all over the propagation area with grid lengths of $\Delta x = \Delta y = 0.2$ m, and a refined grid of 0.1 m close to the breach zone. Within the channel detection was performed at different cross sections. Up to eight sensors were mounted on movable cross-beams enabling measurements at various locations.

Vertical velocity profiles $u(z)$, $v(z)$ were sampled using a conventional 1D Laser-Doppler

Anemometer (LDA), mounted on an automatic traversing unit beneath the glass plate. Horizontal velocity components over depth are sampled at three cross-sections y = 0.25, 0.30, 0.35 m near the breach in a dense grid of $\Delta x = 0.05$ m, $\Delta z = 0.01$ m within the wave. These profiles provide a distribution of momentum correction coefficients (BOUSSINESQ coefficients), which may be exploited for 2D numerical modelling.

2.3 *Test configurations*

Four initial hydraulic configurations (Table 1) were considered differing in the discharge at the channel inlet and in the initial channel flow depth. A steady flow was established in the channel, before the gate was opened in each model run. Then, the inflow splits into the breach discharge and the weir overflow from the downstream channel.

Table 1. Test configurations for breach width b = 0.70 m.

Test ID	Inflow [l/s]	Initial depth [cm]	Crest height [cm]
Q300-h50	300	50	24.1
Q300-h40	300	40	15.2
Q200-h50	200	50	29.7
Q200-h50	200	40	20.2

The channel inflow was controlled via an ultrasonic flow-measuring device. A weir at the channel end was calibrated for different crest heights to control the initial water depth. The rating curve for each of those weir positions and the corresponding discharge coefficients were determined experimentally running various known discharges from the inlet while keeping the gate closed. Measuring the water level at the channel end yields the discharge over the weir. Consequently, the steady-state breach discharge Q_B was indirectly calculated as the difference between model inflow and weir overflow Q_w. Figure 2 also shows the different boundary conditions.

3 MATHEMATICAL AND NUMERICAL MODELS

3.1 *Shallow water models*

Firstly, numerical simulations of the experimental flow configurations have been performed with two different 2D models solving the depth-averaged Shallow-Water Equations (SWE). The basic assumption states that velocities normal to the main flow directions remain small. As a consequence the pressure field is hydrostatic, which limits the applicability of the SWE.

On the one hand DGFLOW is applied, a total variation diminishing (TVD) RUNGE KUTTA discontinuous GALERKIN (RKDG) finite element (FE) method on unstructured triangular meshes, developed at IWW, RWTH Aachen University (Schwanenberg & Harms, 2002, 2004). On the other hand WOLF 2D is used, a finite volume (FV) scheme involving a flux vector splitting (FVS) method on a multiblock structured grid, developed at the University of Liege (Erpicum et al., 2010a).

Both schemes are well suited to handle transient, rapidly varying dam-break induced flows with steep gradients over a dry bed. Now they are applied to the dike-break induced flow conditions in the experimental test arrangement. As Roger et al. (2009) describe the computational methods in detail the two following paragraphs and Table 2 only delivers a brief insight.

Table 2. Comparison of the two applied SWE models DGFlow and WOLF 2D.

Characteristics	DGFlow	WOLF 2D
Model type	Finite Element	Finite Volume
Space	Discontious	Flux Vector
Discretisation	GALERKIN (DG)	Splitting (FVS)
Time integration	TVD RUNGE-KUTTA	RUNGE-KUTTA
Numerical grid	Triangular	Cartesian
Number of elements	23,000	60,000
Edge lengths [m]	0.03 – 0.05	0.02
Bottom friction	MANNING	MANNING
Turbulence Closure	None	Algebraic/k-ε
Wall roughness	None	Accounted for
BOUSSINESQ coeff.	Set to unity	Distributed values

3.2 *DGFlow*

DGFlow is based on the RKDG method for hyperbolic equation systems and the local discontinuous Galerkin method for advection-dominated flows (Cockburn 1999, Cockburn et al. 2000). The leadoff implementation of the RKDG method to the SWE was presented by Schwanenberg and Köngeter (2000). The scheme can be divided into three main steps:

- Decoupling the partial differential equations by a DG space discretisation (polynomial degree k) into a set of ordinary differential equations
- Integrating the ordinary differential equations in time by a (k+1)-order TVD RK method
- Applying a slope limiter on every intermediate time step introducing a selective amount of dissipation to obtain stability at shocks

3.3 *WOLF 2D*

WOLF 2D solves the divergence form of the shallow-water equations by means of a finite volume

scheme. Variable reconstruction at cells interfaces is either constant or linear, combined with a slope limiter, leading in the latter case to second-order space accuracy. The fluxes are computed by a self-developed Flux Vector Splitting (FVS) method, in which the upwinding direction of each flux is simply dictated by the sign of the flow velocity reconstructed at the cell interfaces.

A "VON NEUMANN" stability analysis has demonstrated that this FVS leads to a stable spatial discretization, requiring low computational cost. This FVS offers the advantages of being completely Froude-independent and of facilitating a satisfactory adequacy with the discretization of the bottom slope term. The turbulent fluxes are simply evaluated by means of a centred scheme.

The time integration was performed here by means of a 3-step first-order accurate RK algorithm. A semi-implicit treatment of the bottom friction term in was used, without requiring additional computational cost.

Besides, wetting and drying of cells is handled free of mass conservation error by means of an iterative resolution of the continuity equation at each time step. A grid adaptation technique restricts the simulation domain to the wet cells.

This finite volume scheme has already proven its validity and efficiency for numerous applications (Dewals et al., 2008, Erpicum et al., 2009, Erpicum et al., 2010b).

3.4 *Star-CD*

Subsequently, a fully 3D model has been set up: the commercial code Star-CD (CD-adapco, 2005) is based on the REYNOLDS-averaged NAVIER STOKES equations (RANS) and accounts for the free surface location via a volume of fluid method (Table 3).

Table 3. Main characteristics of RANS model Star-CD.

Model type	Finite Volume
Space Discretisation	Upwind Differencing Scheme
Time integration	Implcit scheme
Numerical grid	Triangular prisms
Number of Cells	250,000 – 300,000
Cell dimensions [m]	0.02 – 0.05 m
Bottom friction	wall function
Turbulence Closure	k-ε-model
Wall roughness	wall function

Roughness and turbulence effects are considered via a wall-functional approach and a k-ε-turbulence model, respectively. Once again the different scenarios of the scale model tests are computed in 3D. All results are compared with the measurements and exploited in detail in terms of flow depths, flow velocities, and calculation of the breach discharge. In some cases (dispersion, dissipation), the 3D information is used to estimate appropriate settings for the 2D approaches.

4 NUMERICAL MODELLING

4.1 *Computational procedure and former results*

All numerical simulations of the different experimental configurations reproduce the basic flow pattern satisfactorily (Figure 3), which confirms the convergence and general applicability of the methods on dike-break type of problems. At first the initial state was computed for a closed flap gate which corresponds to a simple steady channel flow with a sharp crested weir at the outflow section. According to the opening mechanism in the scale model tests, an immediate and complete failure of flood protection measures with a rectangular breach was realised in the numerical computations by changing the respective boundary condition at the breach location. Simulations contained the transient propagation and development of the dike break wave in the floodplain as well as the open channel flow. The whole flooding event was modelled, starting from an initial condition until the final steady solution in a single stable run without oscillations.

The resulting deviations from the performed measurements were analysed focussing on the simplifications of the mathematical model or the numerical approach (Roger et al., 2009). The latter has to deal with complex free surface structures or steep gradients. As regards the mathematical models the different simulations enable direct comparisons between the assumptions of the SWE and the less simplified RANS in relation to the collected experimental data.

In addition to the hydraulic (discharge, initial water level) and geometric (breach width) boundary and initial conditions, several numerical parameters were examined. A preliminary study with DGFlow has yielded the required fineness of the numerical grid in order to obtain an almost mesh independent solution and to minimize the discretization error (Roger et al., 2009). A sensitivity analysis was performed as regards bed roughness. Additional simulations were performed with WOLD 2D introducing non-uniform BOUSSINESQ-coefficients (for uneven horizontal velocity distribution over depth) as well as different turbulence closure schemes and wall roughness coefficients to analyze whether these approaches affect the computed 2D solutions compared to the measurements.

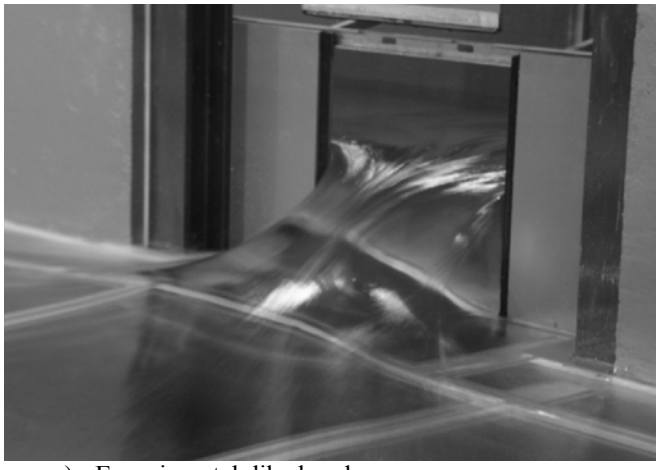

a) Experimental dike break wave.

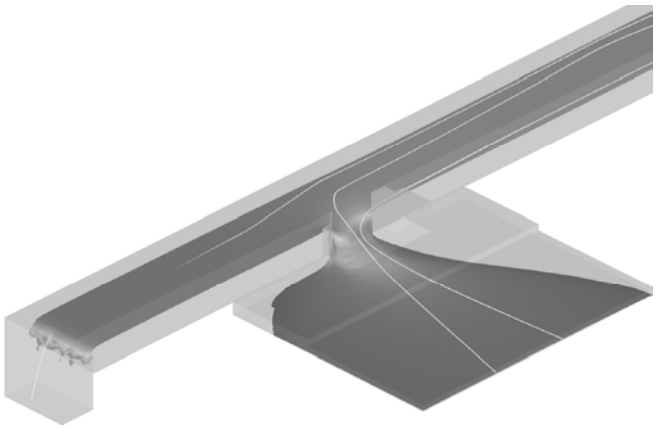

b) Numerical dike break wave (Star-CD).

Figure 3. Experimental (a) and numerical (b) modelling of dike-break induced flow.

4.2 *Boundary conditions*

At the channel inlet (Figure 2), the unit discharge was prescribed as an upstream inflow boundary condition. At the edges of the propagation area (glass plate) no boundary condition was needed for the obtained supercritical outflow.

Specific difficulties occur with respect to the modelling of the flow split into breach discharge and the discharge in the downstream channel. Particularly, in combination with the downstream boundary condition, this additional degree of freedom may lead to numerical problems (Roger et al., 2006). In both 2D codes the calibrated weir formulas for different crest heights (Table 1) were implemented as possible downstream boundary conditions (Roger et al., 2009) while the complete weir has been geometrically discretized for the 3D computations. Thus, the dynamics of the weir discharge depending on the actual channel water level could be modelled properly. The resulting backwater effects interact with the flow resistance of the downstream channel reach compared to the breach section as well as with the flow split into breach discharge and downstream channel discharge. The 90°-turn of momentum from the main channel flow to the breach main axis is closely related to the interplay of flow partition and downstream boundary.

4.3 *Breach discharge*

The large-scale and long-term inundation of a floodplain in practical applications is strongly affected by the steady-state discharge through the breach. Thus, its correct calculation is the decisive parameter to evaluate model modifications. Simulated and measured discharges across the breach are compared in Table 4 and Fig. 4. Though the qualitative flow split for all four configurations is modelled correctly, the 2D-numerical predictions underestimate the discharge released into the floodplain by 6 to 11% of the test breach discharge. Consistently with theoretical hypothesis, the 3D results fit better the scale model data than the shallow water approaches, without succeeding in exactly calculating the breach discharge. The next paragraphs aim at investigating whether this issue can be enhanced in the framework of depth-averaged flow modelling.

Table 4. Measured and computed breach discharges.

Test ID	Measured [l/s]	DGFlow [l/s]	WOLF 2D [l/s]	Star-CD [l/s]
Q300-h50	218	200	198	211
Q300-h40	159	141	141	153
Q200-h50	194	183	182	190
Q200-h50	154	143	141	148

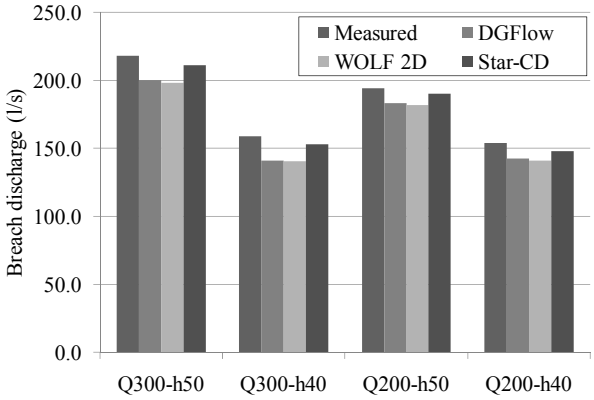

Figure 4. Measured and computed breach discharges.

For test configuration Q300-h50, the simulations were repeated with two types of turbulence closures implemented in WOLF 2D, that is a purely algebraic expression for eddy viscosity and a two-length-scale depth-averaged k-ε model. Moreover, the influence of bed and wall roughness was investigated. As described in Roger et al. (2009) and summarized in Table 5, the turbulence closure as well as bed and wall roughness have basically a minor effect on the computational results.

Table 5. Influence of turbulence and wall-roughness on breach discharges predicted by WOLF 2D.

Test ID	Measured [l/s]	WOLF 2D [l/s]	WOLF 2D Turb[l/s]	WOLF 2D Wall[l/s]
Q300-h50	218	198	198	202-204

4.4 *Velocity profile and pressure distribution*

The 6 to 11% discrepancy between measured values and the breach discharges simulated based on the 2D depth-averaged model is found to remain essentially insensitive to the turbulence closure and the roughness coefficients. This suggests that the difference may result from the basic assumptions inherent to depth-average modelling, such as simplified velocity profile and hydrostatic pressure distribution along the water depth. This was investigated based on the evaluation of BOUSSINESQ coefficients ρ_{xx}, ρ_{yy}, ρ_{xy} and pressure coefficient Λ, defined as follows:

$$\rho_{xx} = \langle u^2 \rangle / \langle u \rangle^2 \quad ; \quad \rho_{yy} = \langle v^2 \rangle / \langle v \rangle^2 \quad ; \\ \rho_{xy} = \langle uv \rangle / (\langle u \rangle \langle v \rangle) \quad ; \quad \Lambda = 0.5 + \langle p/(\rho g h) \rangle \tag{1}$$

where h = flow depth, u, v = local velocity components in x- and y-directions, p = water density, g = gravitational acceleration, ρ = water density and angle brackets representing depth-averaging.

The BOUSSINESQ coefficients are all equal to unity in case of a uniform velocity profile along the water depth, whereas the greater the BOUSSINESQ coefficients the more irregular the velocity profile. In standard shallow-water models, BOUSSINESQ coefficients are all implicitly set to unity. It may be mathematically demonstrated that the value of ρ_{xx} and ρ_{yy}, is never below unity, while ρ_{xy} verifies: $\rho_{xy}\,\rho_{xy} < \rho_{xx}\,\rho_{yy}$. In river flows, BOUSSINESQ coefficients remain usually very close to unity, except if significant secondary flows occur (e.g. in bends). Similarly, the pressure coefficient equals unity in case of hydrostatic distribution and deviates from unity in all other cases.

Here, the velocity and pressure profiles along the water depth computed by Star-CD were used to evaluate the BOUSSINESQ and pressure coefficients by integrating manually the horizontal velocities and the pressure values over water depth. As detailed in Fig. 5, the pattern of BOUSSINESQ coefficients ρ_{xx} reveals mainly two regions of significantly non-uniform velocity profiles, namely in the dike-break wave and at the beginning of the downstream channel reach. The former probably has no influence on flow split because of the supercritical flow in advance. The latter, however, may strongly affect the discharge partition. Considering the 2D-results, the flow resistance of the downstream channel reach tends to be too low compared to the breach section. That might be the reason why too much water goes over the weir instead of entering the floodplain.

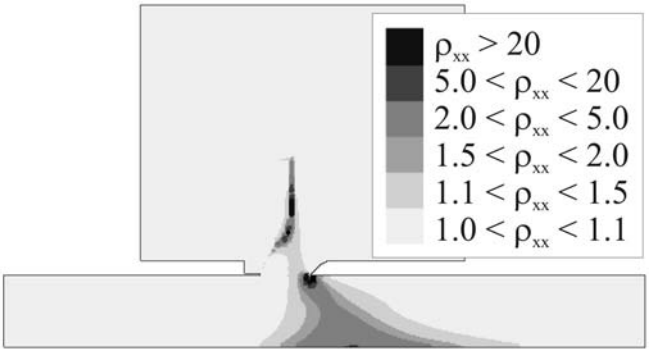

Figure 5. BOUSSINESQ coefficient ρ_{xx}.

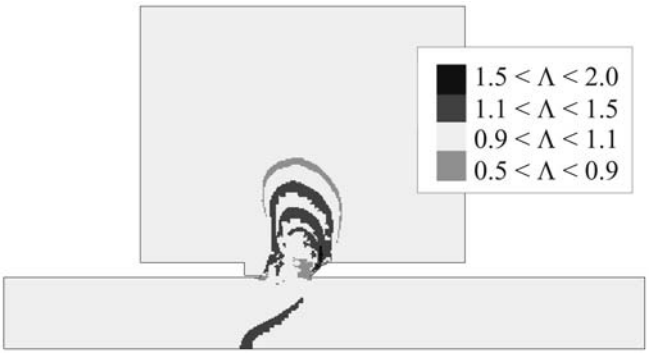

Figure 6. Pressure coefficient Λ.

The pattern of BOUSSINESQ coefficient ρ_{xy} in the downstream channel is found similar to the pattern of ρ_{xx} represented in Fig. 5. Hence, ρ_{xy} reflects a non-uniform profile of flow velocity which also contributes an increase to the effective flow resistance in the downstream channel. This effect is disregarded in the 2D depth-averaged predictions of breach discharge. Although the third BOUSSINESQ coefficient ρ_{yy} also takes values significantly deviating from unity in the channel, it may not be invoked as an explanation for the underestimation of breach discharge. These high values of ρ_{yy} simply result from zero-crossings of the very low depth-averaged transverse velocity components throughout the whole channel.

Finally, the pressure coefficient Λ is represented in Fig. 6. The pressure is found to show an interesting pattern of secondary waves superimposed on the main dike-break wave. Again, this effect does not play a part in the flow split since it is located downstream of the transition from subcritical to supercritical flow. But in a confined region of the channel there are deviations from hydrostatic distribution which also may enlarge the flow resistance for the main channel flow.

5 CONCLUSIONS

Dike-break induced flow has been investigated based on hybrid modeling, involving physical modeling as well as 2D depth-averaged and complete 3D simulations. While the 2D simulations were shown to underestimate the breach discharge, post-processing of 3D results has been successfully used to demonstrate that non-uniform velocity profiles as well as non-hydrostatic conditions near the breach in the channel are most probably the main reasons for this underestimation. Additional simulations introducing a reliable spatial distribution of BOUSSINESQ and pressure coefficients may clarify their respective impact.

ACKNOWLEDGEMENTS

The first author thanks the German Research Foundation (DFG) for funding his research project under reference number KO 1573/15-2.

REFERENCES

Aureli, F., Mignosa, P. 2002. Rapidly varying flows due to levee-breaking. Proc. Intl. Conf. Fluvial Hydraulics (River Flow), Louvain-la-Neuve, Belgium, 1, 459-466

Aureli, F., Mignosa, P. 2004. Flooding scenarios due to levee breaking in the Po river. Water Manage. 157, 3-12.

Aureli, F., Maranzoni, A., Mignosa, P. 2004. Experimental modelling of rapidly varying flows on wet bed and in presence of submersible obstacles. Proc. 2nd Intl. Conf. Fluvial Hydraulics (River Flow), Naples, Italy, 2, 849-858, Balkema, Rotterdam.

Briechle, S., Köngeter, J. 2002. Experimental data for dike-break waves. Proc. Intl. Conf. Fluvial Hydraulics (River Flow), Louvain-la-Neuve, Belgium, 1, 467-473.

Briechle, S., Joeppen, A., Köngeter, J. 2004. Physical model tests for dike-break induced, two-dimensionaol flood wave propagation. Proc. 2nd Intl. Conf. Fluvial Hydraulics (River Flow), Naples, Italy, 2, 959-966, Balkema, Rotterdam.

Briechle, S. 2006. Die flächenhafte Ausbreitung der Flutwelle nach Versagen von Hochwasserschutzeinrichtung an Fließgewässern. Shaker, Aachen [in German].

Brufau, P., Garcia-Navarro, P. 2000. Two-dimensional dam break flow simulation. Int. J. Numer. Methods Fluids, 33(1), 35-57

CADAM 2000. Concerted action on dambreak modeling. Final Report SR 571, HR Wallingford UK.

CD-adapco 2005. Star-CD Version 3.26. Methodology, Commands and User Guide.

Cockburn, B. 1999. Discontinuous Galerkin methods for convection-dominated problems. Lecture Notes in Computational Science and Engineering, 9, 69-224. Springer, Berlin.

Cockburn, B., Karniadakis, G.E., Shu, C.W. 2000. Discontinuous Galerkin methods. Lecture Notes in Computational Science and Engineering 11. Springer, Berlin.

Dewals, B.J., Kantoush, S.A., Erpicum, S., Pirotton, M., Schleiss, A. J. 2008. Experimental and numerical analysis of flow instabilities in rectangular shallow basins. Environ. Fluid Mech. 8, 31-54. DOI: 10.1007/s10652-008-9053-z.

Eaket, J., Hicks, F.E., Peterson, A.E. 2005. Use of Stereoscopy for Dam Break Flow Measurements. Journal of Hydraulic Engineering 131(1), 24-29.

Stelling, G.S., Duinmeijer, S.P.A. 2003. A staggered conservative scheme for every Froude number in rapidly varied shallow water flows. Int. J. Numer. Methods Fluids, 43(12), 1329-1354. DOI: 10.1002/fld.537.

Erpicum, S., Meile, T., Dewals, B.J., Pirotton, M., Schleiss. A. J. 2009. 2D numerical flow modeling in a macro-rough channel. Int. J. Numer. Methods Fluids, 61(11), 1227-1246. DOI: 10.1002/fld.2002.

Erpicum, S., Dewals, B.J., Archambeau, P. and Pirotton, M. 2010a. Dam-break flow computation based on an efficient flux-vector splitting. Journal of Computational and Applied Mathematics, 234(7), 2143-2151.

Erpicum, S., Dewals, B.J., Archambeau, P., Detrembleur, S., Pirotton, M. 2010b. Detailed inundation modelling using high resolution DEMs. Engineering Applications of Computational Fluid Mechanics, 4(2), 196-208.

Fraccarollo, L., Toro, E. 1995. Experimental and numerical assessment of the shallow water model for two-dimensional dam-break type problems. Journal of Hydraulic Research 33(6), 843-863.

Hervouet, J.M., Petitjean, A. 1999. Malpasset dam-break revisited with two-dimensional computations. Journal of Hydraulic Research 37(6), 777-788.

IMPACT 2005. Investigation of extreme flood processes and uncertainty. Final Technical ReportEVG1-CT-2001-00037, HR Wallingford UK.

Kulisch, H. 2002. Ausbreitung von Dammbruchwellen im physikalischen Modell. Oldenbourg, München [in German].

Kutschera, G., Bachmann, D., Huber, N.P., Niemeyer, M., Köngeter, J. 2008. RAPID – Ein Risk-Assessment-Verfahren für den technischen Hochwasserschutz. Wasserwirtschaft 98(1-2), 43-48 [in German].

RESCDAM 2001. RESCDAM - Development of rescue actions based on dam-break flood analysis. Final Report 99/52623, Finnish Environmental Institute, Helsinki, Finland.

Rettemeier, K., Falkenhagen, B., Köngeter, J. 2000. Risk Assessment – New Trends in Germany. Proc. 20th ICOLD Congress, Bejing, China, Vol. 1, 625-641.

Roger, S., Büsse, E., Köngeter, J. 2006. Dike-break induced flood wave propagation. Proc. of the 7th Int. Conf. on Hydroinformatics, Nice, France, 2, 1131-1138.

Roger, S., Dewals, B.J., Erpicum, S., Schwanenberg, D., Schüttrumpf, H., Köngeter, J., Pirotton, M. 2009. Experimental and numerical investigations of dike-break induced flows. Journal of Hydraulic Research 47(3), 349-359; DOI: 10.3826/jhr.2009.3472.

Schwanenberg, D., Harms, M. 2002. Discontinuous Galerkin method for dam-break flows. Proc. Intl. Conf. Fluvial Hydraulics (River Flow), Louvain-la-Neuve, Belgium, 1, 443-448.

Schwanenberg, D., Harms, M. 2004. Discontinuous Galerkin Finite-Element Method for transcritical two-dimensional shallow water flows. Journal of Hydraulic Engineering 130(5), 412-421.

Schwanenberg, D., Köngeter, J. 2000. A discontinuous Galerkin method for the shallow water equations with source terms. Lecture Notes in Computational Science and Engineering 11, 419-424. Springer, Berlin.

Shige-eda, M., Akiyama, J. 2003. Numerical and Experimental Study on Two-Dimensional Flood Flows with

and without Structures. Journal of Hydraulic Engineering 129(10), 817-821.
Toro, E.F. 2001. Shock-capturing methods for free-surface shallow flows. Wiley, Chichester – 0-471-98766-2